Coexpression of the chemokines ELC and SLC by T zone stromal cells and deletion of the ELC gene in the *plt*/*plt* mouse

Sanjiv A. Luther*†, H. Lucy Tang*†, Paul L. Hyman*, Andrew G. Farr‡, and Jason G. Cyster*§

*Department of Microbiology and Immunology and Howard Hughes Medical Institute, University of California, San Francisco, CA 94143; and ‡Departments of Biological Structure and Immunology, University of Washington, Seattle, WA 98195

Communicated by Hugh O. McDevitt, Stanford University School of Medicine, Stanford, CA, September 12, 2000 (received for review June 28, 2000)

The spontaneous mutant mouse strain, *plt*/*plt*, lacks the secondary lymphoid organ chemokine (SLC)-ser gene and has disrupted trafficking of T cells and dendritic cells (DCs) to lymphoid tissues. We demonstrate here that the gene for the related chemokine, Epstein–Barr virus-induced molecule-1 ligand chemokine (ELC), is also deleted in this immunodeficient mouse strain. Using a combination of approaches, including bone marrow reconstitution and double *in situ* hybridization, we show in wild-type mice that ELC is expressed by T zone stromal cells that also make SLC. Smaller amounts of ELC are made by DCs, predominantly of the CD8$^+$ phenotype. We propose that ELC- and SLC-expressing T zone stromal cells play a central role in bringing naive T cells and DCs together for the initiation of immune responses.

The rapid initiation of T cell immune responses depends on efficient encounter between antigen-bearing dendritic cells (DCs) and recirculating T cells. These encounters are promoted by the colocalization of DCs and naïve T cells in lymphoid tissues. Recent studies have indicated that the chemokine receptor CCR7, and its CC chemokine ligands SLC (recently designated CCL21, ref. 1) and ELC (CCL19, also ref. 1), play important roles in directing T cells and DCs into lymphoid T zones (2–6).

ELC and SLC are constitutively expressed by cells distributed throughout the T zone of spleen, lymph nodes (LNs), and Peyer's patches (4–6). In addition, SLC is expressed by high endothelial venules (HEVs) in LNs and Peyer's patches and by lymphatic endothelial cells in most nonlymphoid tissues (4–6). Evidence that SLC plays an essential role in directing T cell and DC movements comes from the discovery that an autosomal recessive mutation in mouse, *p*aucity of *l*ymph node *T* cells (*plt*) (7), correlates with lack of detectable SLC expression in lymphoid organs (3). In these animals, T cell adhesion to HEVs is impaired (8, 9), and T cell entry into LNs is greatly reduced (7). DC numbers in LNs are also low, and skin sensitization studies revealed a marked defect in DC trafficking to LNs via lymphatics (3). T cells and DCs also fail to organize normally in T zones of the spleen (3, 7). Recently, Vassileva and colleagues found two mouse SLC genes encoding mature proteins that differ by a single amino acid and termed the genes SLC-ser and SLC-leu in accord with the products they encode (10). Although the two SLC proteins appear functionally identical, they differ in expression pattern, SLC-ser being expressed in lymphoid tissues and SLC-leu in nonlymphoid tissues. The lymphoid tissue form, SLC-ser, was shown to be genomically deleted in *plt*/*plt* mice (10).

A complication in interpreting the basis for the *plt*/*plt* phenotype was the observation that ELC transcript levels in *plt*/*plt* spleen and LNs were severalfold reduced (3). Since studies in human and mouse established that DCs and macrophages could produce ELC (reviewed in refs. 4–6), one possible explanation for the diminished ELC expression in *plt*/*plt* mice was a defect in accumulation of ELC-expressing cells secondary to the loss of lymphoid SLC expression. However, the knowledge that the SLC and ELC genes are linked on human chromosome 9p13 (11) raised the possibility that *plt*/*plt* mice have a genetic defect in ELC expression.

Here, we report that there are multiple transcribed ELC genes in the mouse genome but only one gene that encodes ELC protein. We show that this gene is deleted in *plt*/*plt* mice. Using bone marrow chimera and cell-sorting approaches, we establish that only small amounts of ELC are made by DCs, whereas the bulk of ELC, as well as SLC-ser, is made by radiation-resistant cells. Double *in situ* hybridization experiments indicate frequent coexpression of ELC and SLC by the same cells. By costaining for SLC and gp38, a cell-surface molecule expressed by most T zone stromal cells (12), we provide evidence that many of the chemokine-expressing cells are gp38$^+$ stromal cells. Our results establish that T zone stromal cells are a major source of T cell and DC chemoattractants, and they suggest a critical role for these cells in fostering interactions between naïve T cells and DCs.

Materials and Methods

Mice. BALB/cAnN, C57BL/6, and B10D2 mice were from Charles River Breeding Laboratories, and 129/sv mice were from the Jackson Laboratory. A breeder pair of *plt*/*plt* mice backcrossed for six generations to the BALB/c strain was kindly provided by H. Nakano and M. Gunn (Duke University Medical Center, Durham, NC) and were maintained by intercrossing. Bone marrow chimeras were generated as described (13). Skin sensitization with FITC was as in ref. 14.

PCR Primers. PCR primer pairs, including their specificity, identification tag, orientation (forward, F; reverse, R), sequence, and product length were as follows: screening of P1 library for ELC-atg (SL06 F exon 1 gcctcagattatctgccat, SL07 R exon 2 atcattagcacccccagag, 1090 bp); Southern probe (SL06 F, SL19 R intron 1 atggagcccacagctataag, 303 bp); semiquantitative PCR: ELC-atg (SL06 F, 3′ELC R agacacagggctccttctggt, 350 bp); ELC-acg (SL21 F gcctcagatcgtctgccac, 3′ELC R, 350bp); SLC (HLT77 F exon 1/2 ccctggacccaaggcagt, SL30 R exon 3/4 agttctcttgcagcccttgg, 320 bp); SLC-ser (SL42 F exon 2/3 atcccggcaatcctgttctc, SL30 R, 200 bp); SLC-leu (SL43 F exon 2/3 atcccggcaatcctgttctt, SL30 R, 200 bp); Dec205 (HLT28 F gttgcacctgtgattggtgg, HLT29 R gggagtcttgttgaagggaac, 450 bp);

Abbreviations: DC, dendritic cell; ELC, Epstein–Barr virus-induced molecule-1 ligand chemokine; EST, expressed sequence tag; LN, lymph node; SLC, secondary lymphoid organ chemokine; HEV, high endothelial venule; DIG, digoxigenin; BCIP, 5-bromo-4-chloro-3-indolyl phosphate.

Data deposition: The sequences reported in this paper have been deposited in the GenBank database (accession nos. AF059208 and AF308159).

†S.A.L. and H.L.T. contributed equally to this work.

§To whom reprint requests should be addressed. E-mail: cyster@itsa.ucsf.edu.

The publication costs of this article were defrayed in part by page charge payment. This article must therefore be hereby marked "*advertisement*" in accordance with 18 U.S.C. §1734 solely to indicate this fact.

CD11c (HLT86 F cctggatagcctttcttctg, HLT87 R tgcacagtaggaccacaagc, 320 bp); gp38 (HLT84 F ctctggtaccaacgcagaga, HLT67 R ttagggcgagaaccttcca, 320 bp); HPRT (F gttggatacaggccagacttgttg, R gagggtaggctggcctatggct 350 bp); quantitative PCR: ELC-atg (HLT72 F ctgcctcagattatctgccat, HLT73 R tcattagcaccccccagagt, probe, tggaccttcccagccccaactctg); ELC-acg (SL21 F, HLT73 R, probe as for ELC-atg); SLC (HLT77 F ccctggaccaaggcagt, HLT75 R aggcttagagtgcttccggg, probe, tcccatcccggcaatcctgttctc); HPRT (HLT78 F aggttgcaagcttgctggt, HLT79 R tgaagtactcattatagtcaagggca, probe, tgttggatacaggccagactttgttggat). Analytical PCR conditions were as follows: 94°C for 5 min; 30 cycles of 60°C for 45 s, 72°C for 1 min, 94°C for 45 s; and 72°C for 10 min. Quantitative RT-PCR was performed on an ABI 770 sequence detection instrument (TaqMan) using TaqMan PCR core reagent kit (Perkin–Elmer) following the manufacturer's instructions. Expression was quantified using HPRT as a reference.

ELC-Expressed Sequence Tag (EST) and Genomic Analysis. All ELC EST sequences were obtained from GenBank using EST AA444730 (15) as template and the BLAST program for homology searches and multiple sequence alignments. During reanalysis of this EST, we discovered three sequence errors in the reported (15) 3′-untranslated region (669G, 692T, and 707T should be 669A, 692A, and 707C). Of six further ESTs identified, one (AA245687) corresponded to the previously described cDNA, and five (AI172790, AA265632, AA168274, AA839365, and AA537424) had ACG in place of the ATG start codon plus 4–10 additional nucleotide changes. P1 clones P1–38, -39, -40, and -41 were isolated from the Incyte Pharmaceuticals (Palo Alto, CA) mouse 129/sv P1 library by screening with primers specific for SLC and were kindly provided by M. Gunn (Duke University, Durham, NC). The same library was screened for ELC-atg genes by PCR using primers SL06 and SL07 and led to isolation of P1–364. The ELC gene from P1–364 was subcloned into pBluescript (Stratagene) and sequenced.

Western Blot Analysis. A pool of LNs and spleen was homogenized in ice-cold lysis buffer (120 mM NaCl/50 mM Tris, pH 8.0/1 mM EDTA/6 mM EGTA/1% Nonidet P-40) containing protease inhibitors (1 mM PMSF/1 mM benzamidine/5 μg/ml Leupeptin/5 μg/ml apoprotin). Sepharose CL-4B preabsorbed lysates were incubated with heparin-Sepharose (Amersham Pharmacia); after rotating for 1 h at 4°C, the Sepharose was washed three times and boiled in reducing sample buffer. Western blotting was with goat anti-mouse ELC or SLC (R & D Systems) followed by anti-goat horseradish peroxidase (Jackson ImmunoResearch), and development was with ECL Plus (Amersham Pharmacia). Specificity was controlled by showing lack of reactivity of the ELC- and SLC-specific antibodies with SLC and ELC protein, respectively.

Cell Purification. The spleen samples and DCs used for ELC expression analysis were prepared as described (14). For sorting, DCs were metrizamide enriched from ≈50 collagenase type IV (Worthington) treated C57BL/6 spleens (14), stained with CD11c-FITC, CD3-PE (PharMingen), B220-PE, and CD8α-TC (Caltag, South San Francisco, CA), and CD8α^+ or CD8α^- CD11c$^+$B220$^-$CD3$^-$ cells were purified to >97% using a FACsStar plus (Becton Dickinson). B cells were identified with anti-B220 and sorted to 99% purity. Total RNA was extracted using Trizol (GIBCO/BRL), and about 1 μg was reverse transcribed for 1 h at 42°C using Advantage RT-for-PCR kit (CLONTECH).

Immunohistochemistry. Seven to eight-micrometer frozen sections were acetone fixed for 10 min and air dried. For double staining, anti-SLC antibody (R & D Systems) was applied first, followed by biotinylated donkey anti-goat IgG (The Jackson Laboratory) and alkaline phosphatase-coupled streptavidin-ABC (Vector Laboratories), and then developed with Fast Blue (Sigma)/Naphthol AS-MX. Sections were blocked with RPMI 1640 supplemented with 1 μg/ml dBiotin (Sigma) and 5% goat serum. After washing, sections were stained with hamster anti-mouse gp38 (12), mouse anti-I-A^p (PharMingen), or sheep anti-IgD (The Binding Site, San Diego, CA) followed by horseradish peroxidase-coupled anti-hamster IgG (Jackson ImmunoResearch), streptavidin (Amersham Pharmacia), or anti-sheep IgG (Southern Biotechnology Associates). The peroxidase reaction was developed with diaminobenzidine (Sigma)/H_2O_2. In control experiments, preabsorption of the anti-SLC antibody with SLC was found to block staining.

***In Situ* Hybridization.** Frozen LN sections (5 μm) were air dried, fixed in 4% paraformaldehyde, washed in PBS, prehybridized for 1–4 h, and hybridized overnight at 60°C with sense or antisense digoxigenin (DIG)- or FITC-labeled riboprobes in hybridization solution (15). After washing at high stringency, sections were incubated with sheep anti-DIG antibody (Boehringer Mannheim) followed by alkaline phosphatase-coupled donkey anti-sheep antibody (Jackson ImmunoResearch) and developed with nitroblue tetrazolium/5-bromo-4-chloro-3-indolyl phosphate (BCIP) for blue color, or were incubated with alkaline phosphatase-coupled anti-FITC antibody (Boehringer Mannheim) and developed with 2-(4-iodophenyl)-5-(4-nitrophenyl)-3-phenyl tetrazolium chloride (INT)/BCIP for red color. In the case of double *in situ* hybridization, DIG- and FITC-labeled probes were mixed and hybridized to sections together. The DIG-labeled probe was developed using nitroblue tetrazolium/BCIP, and the sections were then washed in PBS and incubated in TE buffer at 85°C for 10 min to inactivate alkaline phosphatase. The FITC-labeled probe was then stained and developed with INT/BCIP.

Results

Identification of Multiple Mouse ELC Genes but Only One with an ATG Start Codon. During an analysis of the mouse EST database, we observed the presence of multiple C57BL/6-derived ELC cDNA sequences that differed from the characterized cDNA (15) at several positions. In particular, five of seven ESTs contained ACG in place of the ATG initiation codon while otherwise having >98% identity to the characterized sequence. To determine whether these cDNAs corresponded to distinct genes, we analyzed five ELC-containing P1 clones isolated from a 129/sv mouse genomic library. PCR and sequence analysis showed that one clone contained an ELC gene having an ATG start codon, whereas the others contained ELC with ACG in place of the ATG start codon. Similar to other CC-chemokine genes, the ELC-atg gene contained four exons, with three of the four cysteine residues encoded in exon 2 (Fig. 1*A*). PCR analysis of the ELC-acg genes on the other P1s showed they had a comparable organization (Fig. 1*A*). To further investigate the presence of ELC-atg and ELC-acg genes in the mouse genome, we made use of an *Nco*I restriction site that is disrupted by the change of ATG to ACG (Fig. 1*A*). Southern blot analysis of *Nco*I-digested P1 DNA with an ELC probe revealed the expected ≈2.8-kb band in the ELC-atg containing P1 clone (P1–364) and a ≈5-kb band in P1–40 and other P1 clones containing the ELC-acg sequence (Fig. 1*B* and data not shown). Analysis of genomic DNA from 129/sv, C57BL/6, and BALB/c mice showed that each strain contained both the 2.8- and 5-kb bands (Fig. 1*B*), indicating the presence of both ELC-atg and ELC-acg genes. Quantitative analysis of the 2.8- and 5-kb bands in several samples of 129/sv and C57BL/6 DNA suggested the presence of three to four ELC-acg genes and a single ELC-atg gene.

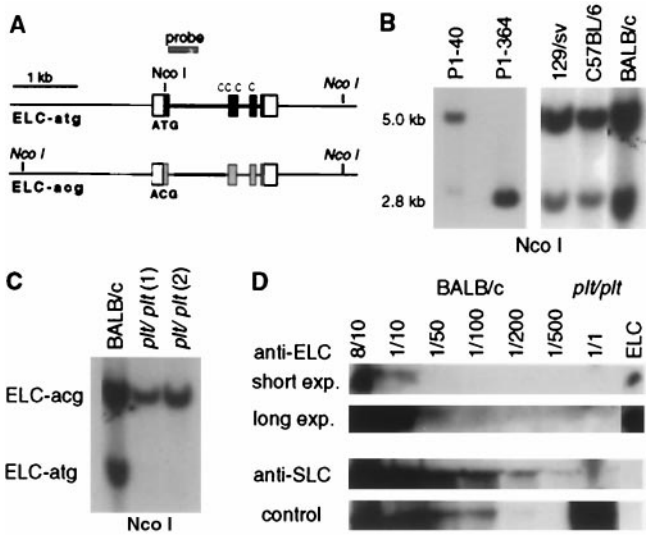

Fig. 1. Genomic analysis of the murine ELC locus shows the presence of one ELC-atg gene and several ELC-acg genes and deletion of the ELC-atg gene in *plt*/*plt* mice. (*A*) Genomic organization of ELC-atg and ELC-acg genes. White boxes show 5′- and 3′-untranslated sequences, black boxes the coding sequence for ELC-atg, and gray boxes the corresponding regions of ELC-acg. The positions of *Nco*I restriction sites are indicated, with the location of sites in italics based upon Southern blot analysis only. (*B*) Southern blot of *Nco*I-digested P1 DNA and mouse genomic DNA to identify ELC-atg (≈2.8 kb) and ELC-acg genes (≈5.0 kb). (*C*) *plt*/*plt* mice lack the ELC-atg gene. Southern blot of *Nco*I-digested DNA from one BALB/c and two *plt*/*plt* mice. The probe used in *B* and *C* is indicated in *A*. (*D*) Western blot of extracts from pooled LNs and spleen from wild-type (BALB/c) or *plt*/*plt* mice, probed with antibodies to ELC or SLC. Extracts from BALB/c mice were titrated from 8 of 10 (80%) to 1 of 500 (0.2%). Short and long exposures of the anti-ELC probed blot are shown. A nonspecific high molecular weight band detected with the anti-ELC serum is shown as a loading control.

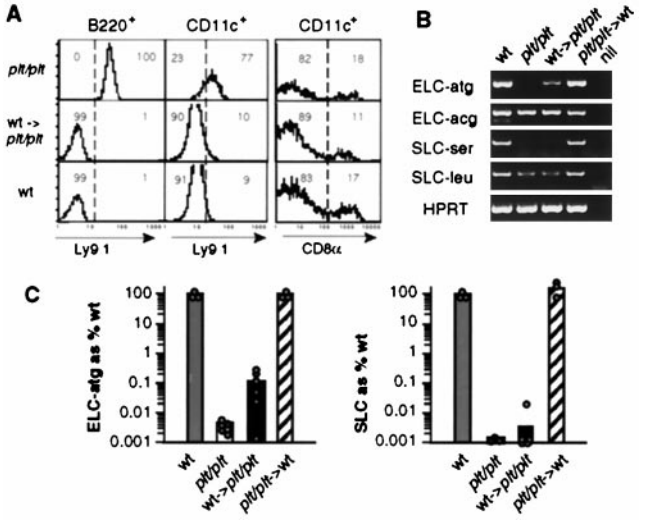

Fig. 2. Partial restoration of ELC but not SLC mRNA expression in spleen of *plt*/*plt* mice that have been reconstituted with wild-type bone marrow. (*A*) Flow cytometric analysis of splenocytes from Ly9.1$^+$ *plt*/*plt* mice, Ly9.1$^-$ B10D2 wild-type mice (wt), or irradiated *plt*/*plt* mice that had been reconstituted with wild-type bone marrow (wt →*plt*/*plt*). Left histograms show Ly9.1 on B cells (B220$^+$), and central histograms show Ly9.1 on DCs (CD11c$^+$B220$^-$CD3$^-$). Right histograms display the proportions of CD11c$^+$ cells that express CD8α. Numbers indicate the percentage of cells in the gated population. The data are representative of at least four mice of each type. (*B*) RT-PCR analysis of ELC and SLC mRNA expression in spleen of wild-type (wt), *plt*/*plt*, and bone marrow chimeric mice. Total spleen RNA from the indicated mice was analyzed by RT-PCR with primers specific for ELC-atg, ELC-acg, SLC-ser, SLC-leu, and HPRT. (*C*) Real-time quantitative RT-PCR analysis of ELC-atg and total SLC expression in samples of the same type as in *B*. Each dot represents an individual mouse, and bars represent the mean.

***plt*/*plt* Mice Lack the ELC-atg Gene and ELC Protein.** Our finding of multiple transcribed ELC genes, together with the knowledge that the ELC and SLC genes are closely linked (11), prompted us to consider whether the reduced amount of ELC mRNA in *plt*/*plt* mice (3) was caused by deletion of one or more of the ELC genes. Strikingly, Southern blot analysis of *Nco*I-digested *plt*/*plt* genomic DNA showed that the 2.8-kb band characteristic for the ELC-atg gene was absent (Fig. 1*C*). No evidence for another band besides the 5-kb band was obtained in *plt*/*plt* mice, whereas both the 2.8- and 5-kb bands could be detected in BALB/c controls (Fig. 1*C*). By Western blot, ELC was undetectable in extracts from *plt*/*plt* spleen and LNs, whereas it could be detected in extracts from wild-type spleen and LNs, even after 50-fold dilution (Fig. 1*D*). Therefore, although there are some reports of low-level translation from ACG codons (16), our findings indicate that there is no detectable translation from the ELC-acg gene(s) in *plt*/*plt* mice. These animals are therefore null for ELC. Analysis of the lymphoid extracts for SLC established, as expected from the previous mRNA analysis (3), that little of this protein could be detected in *plt*/*plt* lymphoid tissue (Fig. 1*D*). In summary, *plt*/*plt* mice lack the ELC-atg and SLC-ser genes and, as a result, are double-deficient for ELC and SLC protein in lymphoid tissues.

ELC and SLC Expression by Radiation-Resistant Cells. To characterize the cell types producing ELC and SLC, we asked whether it was possible to restore expression of these chemokines in secondary lymphoid organs of *plt*/*plt* mice by bone marrow transfer. Bone marrow chimeras were generated by transferring Ly9.1$^-$ wild-type bone marrow into lethally irradiated Ly9.1$^+$ *plt*/*plt* recipients (wt→*plt*/*plt*). Analysis of Ly9.1 expression on B220$^+$ cells and CD11c$^+$ cells established that recipient B cells and DCs had been efficiently replaced by donor-derived cells (Fig. 2*A*). The number of DCs in spleens of *plt*/*plt* mice was in the normal range, as previously reported (3), and this was also the case in the wt→*plt*/*plt* chimeras. We also found that these animals had a wild-type ratio of CD8$^+$ to CD8$^-$ DCs (Fig. 2*A*). RT-PCR analysis of RNA from lymphoid organs of the wt→*plt*/*plt* chimeric mice established that a small amount of ELC-atg mRNA was restored (Fig. 2*B*). In contrast, there was no restoration of SLC-ser mRNA expression (Fig. 2*B*). Surprisingly, some low level expression of SLC-leu was found in lymphoid tissues (Fig. 2*B*), which has not been detected previously by Northern blot analysis (3, 10). As expected from the genetic studies (Fig. 1*C*), ELC-acg pseudogene transcripts were readily detected in *plt*/*plt* mice and were not noticeably altered by bone marrow replacement (Fig. 2*B*). Quantitative PCR analysis showed that the reconstituted ELC-atg expression in chimeric spleen was between 0.1 and 1% of that in wild-type spleen (Fig. 2*C*), whereas there was no restoration of SLC expression (Fig. 2*C*).

One possible explanation for the low reconstitution of ELC-atg in wt→*plt*/*plt* chimeric mice was that the lack of endogenous SLC and ELC in the recipient limited the ability of appropriate hematopoietic cells (such as DCs) to be recruited to the spleen, causing an underestimate of the normal hematopoietic contribution to chemokine expression. The efficient reconstitution of the *plt*/*plt* spleen by donor lymphocytes and CD11c$^+$ cells (Fig. 2*A*) argued against this possibility. As a further approach to test hematopoietic contribution to chemokine expression, reciprocal chimeras were made, where *plt*/*plt* bone marrow was used to reconstitute irradiated wild-type recipients (*plt*/*plt*→wt). De-

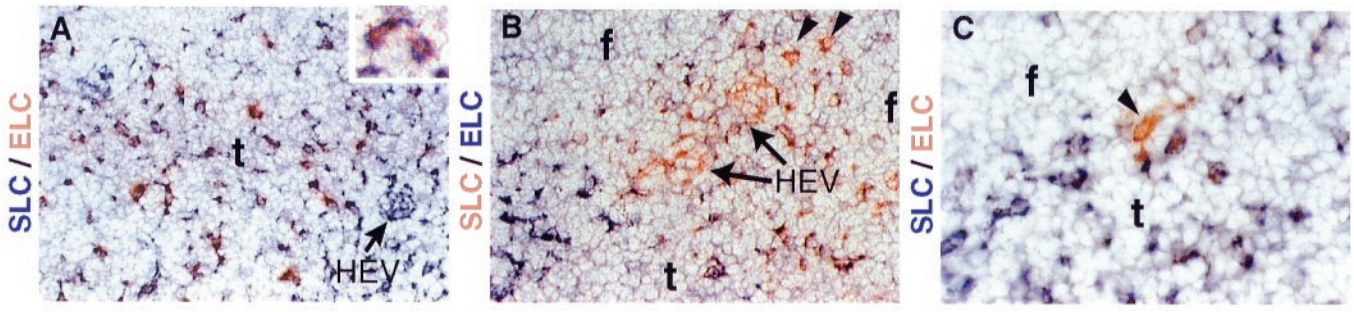

Fig. 3. Coexpression of ELC and SLC in LN T zone. (*A–C*) Bright-field micrographs showing hybridization of mouse LN with the following antisense probes: (*A* and *C*) DIG-labeled SLC probe (blue) and FITC-labeled ELC probe (red); (*B*) DIG-labeled ELC probe (blue) and FITC-labeled SLC probe (red). *Inset* in *A* shows examples of ELC/SLC double-positive cells. In *B* and *C*, the blue reaction product is overdeveloped so that double-positive cells are not visible, but red single-positive cells are apparent. f, follicle; t, T zone. Arrowheads show examples of single-positive cells. (Magnification: *A* and *B*, ×20; *C*, ×40.)

spite flow cytometric confirmation that the majority of lymphocytes and DCs in the reconstituted animals were derived from the *plt/plt* donor (not shown), semiquantitative and quantitative PCR analysis demonstrated little or no reduction in ELC-atg and SLC expression (*plt/plt*→wt; Fig. 2 *B* and *C*). These findings are in agreement with the results in the wt→*plt/plt* chimeras that 0.1–1% of the functional ELC transcripts in spleen are made by bone marrow-derived cells and that the bulk of ELC, and possibly all of the SLC-ser, is made by radiation-resistant cells that most likely are not bone marrow derived.

Coexpression of ELC and SLC by T Zone Cells. Previous *in situ* hybridization studies have shown extensive expression of ELC and SLC throughout the T zone of secondary lymphoid organs. To determine whether ELC and SLC are produced by exclusive or overlapping subsets of cells, we performed double *in situ* hybridization analysis (Fig. 3). Although the ELC probe is unable to distinguish the functional and nonfunctional ELC transcripts, semiquantitative RT-PCR analysis with gene-specific primers indicated that more than half of the total ELC signal in C57BL/6 spleen was from the ELC-atg gene (data not shown). Strikingly, the double *in situ* hybridization analysis revealed a large fraction of cells staining with both *in situ* probes, establishing that many cells coexpress SLC and ELC (Fig. 3*A*). HEVs were positive for SLC but not ELC (Fig. 3 *A* and *B*), as expected (15, 17). In addition, SLC single-positive cells were sometimes present at the border between T zone and follicles and in interfollicular regions (Fig.3*B*). A small number of ELC single-positive cells were also identified (Fig.3*C*), perhaps corresponding to the ELC-producing cells shown in the bone marrow chimera studies (Fig. 2) to be of hematopoietic origin.

Chemokine Expression in Stromal Cells and DCs. As the above studies indicated that ELC and SLC were made predominantly by radiation-resistant cells, we tested whether chemokine transcripts were present in spleen preparations enriched for stromal cells (Fig. 4*A*). When cells are teased from spleen tissue by mechanical mashing, it is thought that most of the hematopoietic cells are released into suspension, whereas collagen fiber-associated stromal cells and other tightly adherent cells remain as a clump of nonsuspendable material. To determine the extent of stromal cell depletion or enrichment in suspendable and nonsuspendable spleen fractions, we measured levels of the stromal cell marker, gp38 (12). Compared with RNA prepared from total spleen, gp38 was depleted in the cell suspension and enriched in the spleen stroma preparation (Fig. 4*A*). Analysis of ELC-atg and SLC transcript levels showed a very similar trend, with strong enrichment in the spleen stroma preparation (Fig. 4*A*). To measure ELC expression in DCs, splenic $CD8^+$ and $CD8^-$ DCs were FACS sorted from collagenase-digested spleen tissue. B and T lymphocytes have previously been shown to lack expression of ELC (15), and FACS-sorted B cells were used as a negative control. RT-PCR analysis for CD11c and DEC205 showed the expected enrichment for these markers in the DC populations, with $CD8^+$ DCs expressing greater amounts of DEC205 than $CD8^-$ DCs (Fig. 4*B*). DEC205 transcripts were also detected in B cells (Fig. 4*B*), consistent with a previous report that B cells express DEC205 protein (19). ELC-atg was detectable in both DC populations, but not in B cells (Fig. 4*B*), and quantitative analysis indicated $CD8^+$ DCs express ≈5-fold greater amounts than $CD8^-$ DCs (Fig. 4*C*). In agreement with the bone marrow chimera studies (Fig. 2), quantitative RT-PCR indicated that DCs account for only a small fraction of the

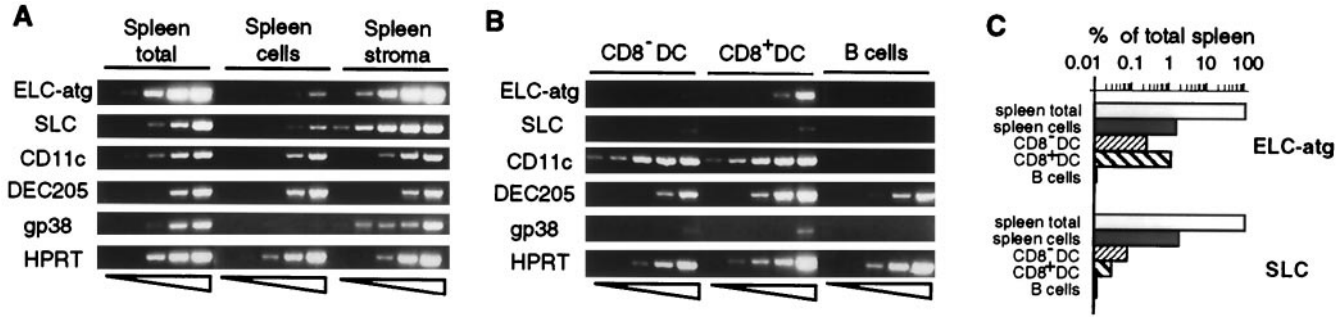

Fig. 4. ELC and SLC mRNA expression in spleen stromal cells and DCs. (*A* and *B*) Semiquantitative RT-PCR for the indicated transcripts using RNA extracted from the following: (*A*) total spleen tissue, a suspension of spleen cells obtained after mechanical mashing of spleen through a cell strainer and the remaining nonsuspendable fraction (spleen stroma); (*B*) sorted $CD8\alpha^-$ and $CD8\alpha^+$ DCs ($CD11c^+B220^-CD3^-$) and sorted B cells ($B220^+$). In *A* and *B*, serial 1:5 dilutions of each cDNA sample were used as template in PCR. (*C*) Quantitative RT-PCR analysis of ELC-atg and SLC expression in samples prepared as in *A* and *B*. Expression is plotted as % of corresponding mRNA in the total spleen.

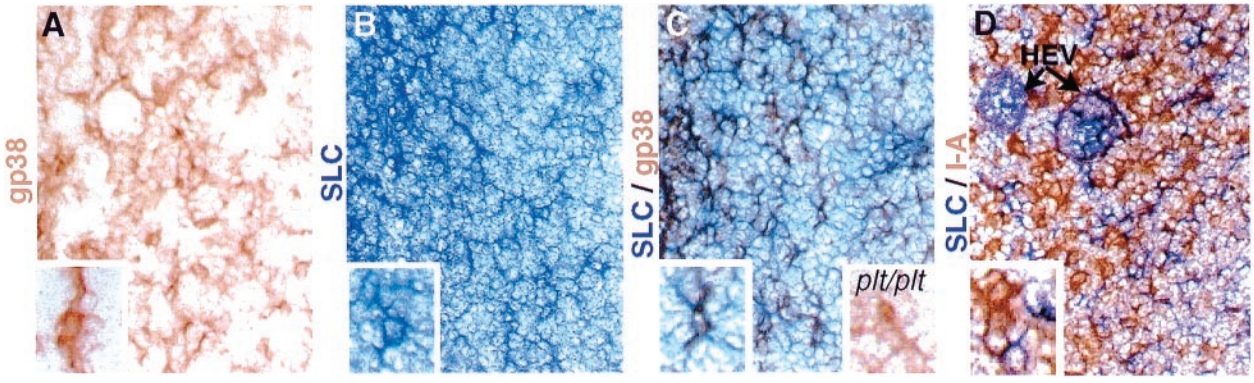

Fig. 5. Distribution of SLC protein with respect to stromal cells and DCs. Immunohistochemistry on serial C57BL/6 LN sections for the stromal cell marker gp38 (*A* and *C*, in brown), for SLC (*B, C*, and *D*, in blue), or for I-A (*D*, in brown). *Insets* in lower left of each image show enlarged views of cells from the same tissue section. *Inset* in lower right of *C* shows a region of *plt/plt* LN stained identically to the wild-type tissue section shown in this panel. (Magnification: ×20.)

ELC-atg signal present in total spleen (Fig. 4*C*). It should be noted that although the DC preparations were greater than 97% $CD11c^+$, the presence of a positive PCR reaction product for gp38 suggests that some contaminating stromal cells may be present (Fig. 4*B*). However, the gp38 signal is similar in the $CD8^-$ and $CD8^+$ preparations, and it is therefore most likely that the greater ELC-atg expression in the $CD8^+$ fraction is a result of expression by $CD8^+$ DCs. Analysis of SLC indicated little or no expression in DCs (Fig. 4 *B* and *C*).

Distribution of SLC Protein in Lymphoid Tissues. To further characterize the relationship between stromal cells and chemokine-expressing cells, we stained sections for gp38 and SLC protein (Fig. 5 *A–C*). Staining for ELC so far has not been successful (not shown). As previously reported (12), anti-gp38 stains the extensive network of collagen fiber-associated stromal cells distributed throughout the lymphoid T zone (Fig. 5*A*). Immunohistochemical analysis of SLC showed strong staining on HEVs (not shown and Fig. 5*D*) and reticular networks in the T zone (Fig. 5*B*). The strong SLC protein staining was comparable to the SLC RNA expression pattern (17), whereas a weaker level of protein staining was detectable throughout the T zone. When the gp38 and SLC stains were combined, the most intense SLC staining was found associated with $gp38^+$ cells (Fig. 5*C*), and the morphology of these cells was often similar to the SLC/ELC double-positive cells identified by *in situ* hybridization (Fig. 3*A*). A similar pattern of gp38 and SLC costaining was found in the T zone of spleen (data not shown). Interestingly, the central arteriole in the spleen was positive for SLC protein (data not shown). All of the SLC staining was specific, as it was not found in tissues from *plt/plt* mice (Fig. 5*C*, *Inset* at bottom, right). In contrast to the overlap between SLC and gp38 staining, I-A and SLC costaining showed there was little overlap (Fig. 5*D*), supporting the notion that $gp38^+$ stromal cells express SLC, whereas MHC class II^+ DCs do not.

Colocalization of DCs with Chemokine-Producing Cells. Although the SLC and I-A costaining showed these molecules did not strongly overlap, MHC class II^+ DCs were frequently in close proximity to SLC^{hi} cells (Fig. 5*D*). Similarly, double *in situ* hybridization analysis for ELC and I-Aβ showed little overlap between the hybridization signals, but I-Aβ^+ DCs and ELC^+ I-Aβ^- cells could be found in close physical association (Fig. 6*A*). As an approach to examine whether antigen-carrying DCs that migrate into LNs come into contact with ELC-producing cells, we performed FITC-contact sensitization experiments (14). Combined fluorescence and *in situ* hybridization analysis of skin-draining LNs 1 day after sensitization revealed the presence of $FITC^+$ DCs adjacent to ELC-expressing cells (Fig. 6*B*), establishing that antigen-bearing DCs can migrate into close physical proximity to chemokine-producing T zone stromal cells.

Discussion

The above findings demonstrate the existence of multiple transcribed ELC genes in the mouse and show that only one, ELC-atg, encodes a functional mRNA that can be translated into protein. The *plt/plt* mouse strain lacks the ELC-atg gene and does not produce detectable ELC protein, leading us to conclude that *plt/plt* mice are ELC deficient. T zone stromal cells are shown to be major producers of ELC and SLC, with many cells coexpressing both chemokines. These studies help explain the close similarity of the phenotype of *plt/plt* mice (3) and CCR7-deficient mice (2). Furthermore, they suggest that attraction by stromal cells is a major mechanism that promotes recruitment of DCs and naïve T cells into the T zone and most likely enhances their encounters.

The presence of multiple linked ELC and SLC genes in the mouse indicates there have been recent gene duplication events in this region of the genome. Although these events have given rise to at least two functional SLC genes (10), the repeated copies of the ELC gene have lost their ATG initiation site. Few functional murine or human genes have been described with start codons other than ATG (16), and the translational inactivity of the ELC-acg pseudogenes is supported by the lack of detectable

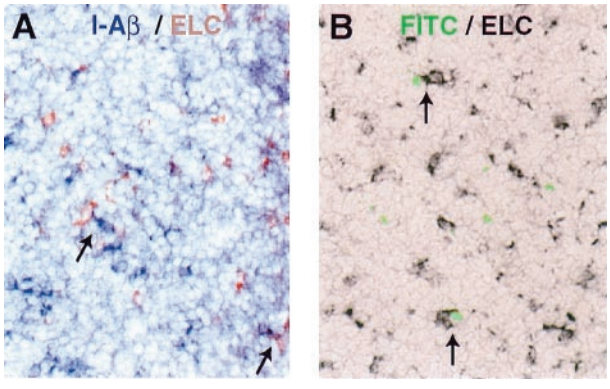

Fig. 6. Close proximity of ELC-producing cells and DCs. (*A*) Double *in situ* hybridization of LN for I-Aβ (blue) and ELC (red). (*B*) Section from the draining LN of a FITC skin-painted mouse, taken at day 1 after painting. Newly immigrated DCs are identified by strong intracellular FITC fluorescence (green) and ELC mRNA-expressing cells by *in situ* hybridization (black). Arrows show examples of colocalizing cells. (Magnification, ×20.)

ELC protein in *plt/plt* mice (Fig. 1). Based on the close proximity of the SLC and ELC loci, it seems likely that *plt/plt* mice have a large deletion in the ELC/SLC locus that encompasses both the ELC-atg and SLC-ser genes but spares the SLC-leu and one or more ELC-acg pseudogenes. These findings necessitate a reconsideration of the relative roles of SLC and ELC in leukocyte trafficking. Each of the reported phenotypes in *plt/plt* mice, including the inefficient trafficking of T cells across HEVs, the inefficient migration of DCs into LNs, and the lack of T cell and DC organization in splenic T zones, could reflect a requirement for SLC, ELC, or both chemokines. Future studies in mice selectively lacking ELC or SLC will be necessary to isolate the roles of the individual chemokines in these processes.

Initial studies on ELC established that it was expressed by *in vitro* generated DCs as well as DCs isolated from lymphoid tissue (15, 18, 20), and this supported a model where DC–naïve T cell interactions are promoted by the DCs directly attracting naïve T cells. DCCK1/PARC has also been suggested to contribute to such a process, although it is a much weaker naïve T cell attractant than ELC (21), and there may not be a gene corresponding to DCCK1 in the mouse genome (22). In other studies, when FITC-bearing Langerhans' cells were followed as they migrated from skin to draining LNs, they did not express ELC and were ineffective *in vitro* in attracting naïve lymphocytes (14). Our findings demonstrate that the functional ELC gene is expressed in DCs, with $CD8^+$ DCs expressing greater amounts than $CD8^-$ DCs. Overall, however, DCs account for only a very small amount of the total ELC (and little or none of the SLC) in lymphoid tissues from unimmunized mice. Instead, both chemokines are produced in large amounts by T zone stromal cells. Although further work is needed to determine to what extent *in vivo* activated DCs up-regulate naïve T cell attractants, current data lead us to propose a model where attraction by stromal cells, rather than DCs, acts as the predominant mechanism responsible for bringing naïve T cells and DCs into physical contact.

T zone stromal cells have so far been relatively poorly characterized. Ultrastructurally, they have mesenchymal characteristics and are closely associated with the supporting collagenous fibers of the tissue (23). Because of their fixed location, it was proposed that T zone stromal cells are well placed to foster interactions between trafficking leukocytes (24), possibly forming migrational "corridors," along which leukocytes must travel as they pass through the T zone (25). Our finding that many T zone stromal cells produce ELC and SLC indicates that migration into these corridors might be actively promoted by the stromal cells themselves. In *in vitro* chemotaxis studies, mature DCs show greater dose sensitivity for ELC and SLC than T cells (26). Perhaps this enables DCs to migrate past T cells to reach close contact with the stromal cells. As naïve T cells migrate along the stromal cell-lined corridors, they are likely to have to migrate over the associated DCs, ensuring extensive DC–T cell contact. It is interesting to note that lymphoid follicles contain stromal cells that are ultrastructurally similar to the cells in T zones (27, 28). Recent studies have provided evidence that many of the follicular stromal cells produce the B cell attractant, BLC (29, 30). Our finding that ELC and SLC are coexpressed by T zone stromal cells highlights the ability of lymphoid stromal cells to acquire specialized properties and suggests an intriguing functional parallel between follicular and T zone stromal cells: both attract naïve lymphocytes and both associate with antigen and display it in a form appropriate for the lymphocytes to recognize. Follicular stromal cells display antigen as immune complexes for recognition by the BCR on BLC-recruited B cells; T zone stromal cells display antigen-bearing DCs for recognition by the TCR on ELC/SLC-recruited T cells.

We thank M. Gunn and H. Nakano for providing the *plt/plt* mice, M. Gunn for P1 clones, and Mark Ansel, Karin Reif, and Steve Rosen for critical reading of the manuscript. This work was supported in part by National Institutes of Health Grant AI45073. S.A.L. was supported by the Swiss National Science Foundation and is presently supported by the Human Frontier Science Program; H.L.T. was supported by the American Lung Association; J.G.C. is a Packard Fellow and an investigator of the Howard Hughes Medical Institute.

1. Zlotnik, A. & Yoshie, O. (2000) *Immunity* **12,** 121–127.
2. Förster, R., Schubel, A., Breitfeld, D., Kremmer, E., Renner-Muller, I., Wolf, E. & Lipp, M. (1999) *Cell* **99,** 23–33.
3. Gunn, M. D., Kyuwa, S., Tam, C., Kakiuchi, T., Matsuzawa, A., Williams, L. T. & Nakano, H. (1999) *J. Exp. Med.* **189,** 451–460.
4. Cyster, J. G. (1999) *Science* **286,** 2098–2102.
5. Zlotnik, A., Morales, J. & Hedrick, J. A. (1999) *Crit. Rev. Immunol.* **19,** 1–47.
6. Sallusto, F., Mackay, C. R. & Lanzavecchia, A. (2000) *Annu. Rev. Immunol.* **18,** 593–620.
7. Nakano, H., Mori, S., Yonekawa, H., Nariuchi, H., Matsuzawa, A. & Kakiuchi, T. (1998) *Blood* **91,** 2886–2895.
8. Stein, J. V., Rot, A., Luo, Y., Narasimhaswamy, M., Nakano, H., Gunn, M. D., Matsuzawa, A., Quackenbush, E. J., Dorf, M. E. & von Andrian, U. H. (2000) *J. Exp. Med.* **191,** 61–76.
9. Warnock, R. A., Campbell, J. J., Dorf, M. E., Matsuzawa, A., McEvoy, L. M. & Butcher, E. C. (2000) *J. Exp. Med.* **191,** 77–88.
10. Vassileva, G., Soto, H., Zlotnik, A., Nakano, H., Kakiuchi, T., Hedrick, J. A. & Lira, S. A. (1999) *J. Exp. Med.* **190,** 1183–1188.
11. Nagira, M., Imai, T., Hieshima, K., Kusuda, J., Ridanpaa, M., Takagi, S., Nishimura, M., Kakizaki, M., Nomiyama, H. & Yoshie, O. (1997) *J. Biol. Chem.* **272,** 19518–19524.
12. Farr, A. G., Berry, M. L., Kim, A., Nelson, A. J., Welch, M. P. & Aruffo, A. (1992) *J. Exp. Med.* **176,** 1477–1482.
13. Cyster, J. G. & Goodnow, C. C. (1995) *Immunity* **3,** 691–701.
14. Tang, H. L. & Cyster, J. G. (1999) *Science* **284,** 819–822.
15. Ngo, V. N., Tang, H. L. & Cyster, J. G. (1998) *J. Exp. Med.* **188,** 181–191.
16. Kozak, M. (1999) *Gene* **234,** 187–208.
17. Gunn, M. D., Tangemann, K., Tam, C., Cyster, J. G., Rosen, S. D. & Williams, L. T. (1998) *Proc. Natl. Acad. Sci. USA* **95,** 258–263.
18. Sallusto, F., Palermo, B., Lenig, D., Miettinen, M., Matikainen, S., Julkunen, I., Forster, R., Burgstahler, R., Lipp, M. & Lanzavecchia, A. (1999) *Eur. J. Immunol.* **29,** 1617–1625.
19. Witmer-Pack, M. D., Swiggard, W. J., Mirza, A., Inaba, K. & Steinman, R. M. (1995) *Cell. Immunol.* **163,** 157–162.
20. Rossi, D. L., Vicari, A. P., Franz–Bacon, K., McClanahan, T. K. & Zlotnik, A. (1997) *J. Immunol.* **158,** 1033–1036.
21. Adema, G. J., Hartgers, F., Verstraten, R., de Vries, E., Marland, G., Menon, S., Foster, J., Xu, Y., Nooyen, P., McClanahan, T., *et al.* (1997) *Nature (London)* **387,** 713–717.
22. Tasaki, Y., Fukuda, S., Lio, M., Miura, R., Imai, T., Sugano, S., Yoshie, O., Hughes, A. L. & Nomiyama, H. (1999) *Genomics* **55,** 353–357.
23. Clark, S. L. (1962) *Am. J. Anat.* **110,** 217–257.
24. Van Vliet, E., Melis, M., Foidart, J. M. & Van Ewijk, W. (1986) *J. Histochem. Cytochem.* **34,** 883–890.
25. Gretz, J. E., Anderson, A. O. & Shaw, S. (1997) *Immunol. Rev.* **156,** 11–24.
26. Kellermann, S. A., Hudak, S., Oldham, E. R., Liu, Y. J. & McEvoy, L. M. (1999) *J. Immunol.* **162,** 3859–3864.
27. Yoshida, K., Tamahashi, N., Matsuura, N., Takahashi, T. & Tachibana, T. (1991) *Cell Tissue Res.* **266,** 223–229.
28. Ushiki, T., Ohtani, O. & Abe, K. (1995) *Anat. Rec.* **241,** 113–122.
29. Gunn, M. D., Ngo, V. N., Ansel, K. M., Ekland, E. H., Cyster, J. G. & Williams, L. T. (1998) *Nature (London)* **391,** 799–803.
30. Ansel, K. M., Ngo, V. N., Hyman, P. L., Luther, S. A., Förster, R., Sedgwick, J. D., Browning, J. L., Lipp, M. & Cyster, J. G. (2000) *Nature (London)* **406,** 309–314.